

# Fractional-Order System Identification for Health Monitoring of Cooperating Robots\*

Kevin Leyden and Bill Goodwine<sup>1</sup>

**Abstract**—Fractional-order differential equations can describe the dynamics of robot formations and other high-order systems. These equations are useful models for such systems because of the ability to include noninteger derivatives. This work presents a procedure to identify the fractional order of a system’s dynamics, which is of interest because the order may change in response to mechanical or operational damage. The possibility of an order change is not typically considered in structural health monitoring or other system monitoring tools; this is because the order is assumed to be an integer from the physics of the system, while behaviors are left to be captured by parameters within the chosen model. In contrast, the inclusion of fractional orders allows for the order itself to measure dynamical changes. This work presents the identification procedure in the form of an explanation of its mathematical foundations, examples matching previously observed results, and a discussion of possible extensions for greater versatility in monitoring.

## I. INTRODUCTION

Consider a group of robots intended to work together in a common space. To be specific, most of the robots must be positioned toward one side of the space to accomplish their task. The best arrangement for this situation could resemble a tree graph, as does the formation in Figure 1. Each generation has twice as many robots as the preceding one. For simplicity, the robots may only translate horizontally;  $x_{ij}$  represents the position of robot  $j$  in the  $i$ th generation. The robots are connected by positional relationships, each behaving as either a spring with constant  $k$  or a damper with constant  $b$ . Previous work [1] shows the fractional-order nature of this system.

Figure 2 is a frequency response showing the transfer function between the position of the first robot,  $x_{11}$ , and that of the last generation,  $x_{last}$ . In other words, the figure shows the amplification in displacement resulting from the force applied to the last (seventh in this case) generation from the spring-damper structure. Under normal circumstances for this formation, all the  $k = 2$ , all the  $b = 1$ , the masses of the first and last generations are 1, and the interior robots have negligible mass. The last of these is enforced so that the spring and damper elements dominate the system. This frequency response is shown in blue.

In Figure 2, the medium-frequency band showing a phase of  $-45^\circ$  and a slope in magnitude of  $-10$  dB/decade suggests  $1/2$ -order dynamics, as explained analytically and

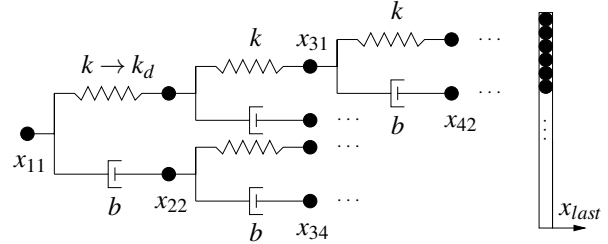


Fig. 1. Structure of robotic formation and spring and damper connections.

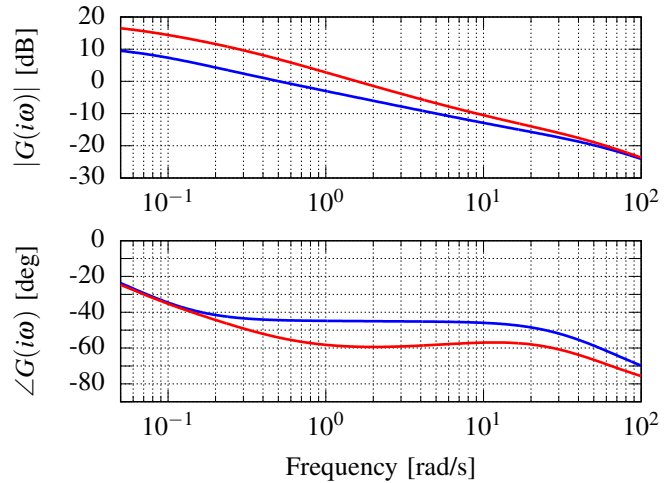


Fig. 2. Frequency responses for undamaged system (blue) and damaged system with  $k_d = 0.2$  (red).

numerically in [1]. Meanwhile, the red curve is the frequency response for the case where there is damage among the interactions comprising the system. All parameters are as in the first case, except that the constant of the spring connecting  $x_{11}$  and  $x_{21}$  takes the value of  $k_d = 0.2$ . Here, the phase plot has a prominent band at  $-60^\circ$ , implying behavior of order  $2/3$ .

This interpretation is supported in [2]. That previous work of the authors suggests that measurement of changes in fractional order could be foundational for health monitoring of complex engineering systems. Applications for this monitoring may include formation problems such as cleanup of toxic waste, as illustrated in Figure 3. This paper contributes a computational identification technique that supports the goal of measuring order changes. The presence of a systematic procedure for detecting these order changes is promising for the development of a widely applicable monitoring tool.

\*The partial support of the US National Science Foundation under the RI Grant No. IIS-1527393 is gratefully acknowledged.

<sup>1</sup>Both authors are with the Department of Aerospace & Mechanical Engineering, University of Notre Dame, Notre Dame, IN 46556 USA, kleyden@nd.edu and bill1@controls.ame.nd.edu

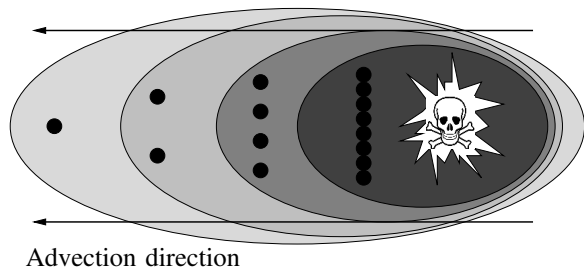


Fig. 3. Sketch of the waste spill example. More robots are placed in more contaminated areas, indicated with darker shading.

## II. BACKGROUND

### A. Literature Review and Research Context

The system in Figure 1, which was inspired by a viscoelastic model from [3], [4], was accurately modeled in [1] by a fractional-order differential equation with a term of order  $1/2$ . Concise models with few terms are advantageous in robotics, and to that end, fractional-order dynamics can be exploited for efficient models of high-order systems such as interacting, multi-agent networks.

For the system monitoring of [2] to evolve into a practical tool, it must be connected to some type of fractional-order system identification. Mathematical works on this topic include [5], which seeks a continuous distribution of real-valued orders to describe a system's behavior. The approach in [6] solves a linear system of equations, resulting in a discrete order distribution. Governing equation parameters can be determined by the series-based method of [7]. Computationally formulated identification procedures include the iterative process described in [8]. Genetic algorithms are employed for optimization of fractional-order governing equations in [9]. The method most compatible with the aims of this work is given in [10]; this method will be explained in detail in the following sections.

The field of control of multi-robot systems is rich with problems of great interest. For a selection of these, see [11]–[16]. Some previous work by the author concerns exact model reduction for systems with symmetries [17]–[20]. Fractional calculus is an area of mathematics dating back near the birth of calculus as a whole. Books on the mathematical fundamentals and engineering applications include [21]–[23], and review articles include [24], [25]. One study along a similar line of inquiry to that in this work is [26], [27], concerning formation control of fractional systems. In those references, the individual components within the system are fractional. Meanwhile, in this paper, the fractional dynamics originate from the structure of the agents' interactions. Additional papers from the authors on fractional calculus in engineering are [28], [29].

### B. Fractional Calculus

Put simply, fractional calculus is the answer to the question of, given a function  $f(t)$  with first derivative  $f^{(1)}(t)$  and second derivative  $f^{(2)}(t)$ , whether there are operators “in

between” these such as

$$f^{(1/2)}(t) = \frac{d^{1/2}f}{dt^{1/2}}(t)$$

that generalize the concept of a derivative beyond the typical integer orders.

While there are closed-form solution techniques for fractional-order differential equations, as overviewed in the authors' prior works and the literature, numerical approximations are often necessary. Consider the following definitions of the first and second derivatives of a function:

$$\begin{aligned} \frac{df}{dt}(t) &= \lim_{\Delta t \rightarrow 0} \frac{f(t) - f(t - \Delta t)}{\Delta t} \\ \frac{d^2f}{dt^2}(t) &= \lim_{\Delta t \rightarrow 0} \frac{f(t) - 2f(t - \Delta t) + f(t - 2\Delta t)}{(\Delta t)^2}, \end{aligned}$$

or for an integer value of  $n$ ,

$$\frac{d^n f}{dt^n}(t) = \lim_{\Delta t \rightarrow 0} \frac{\sum_{0 \leq m \leq n} (-1)^m \binom{n}{m} f(t + (n - m)\Delta t)}{(\Delta t)^n},$$

with the binomial coefficient given by

$$\binom{n}{m} = \frac{n!}{m!(n - m)!}.$$

This can be generalized to any real first argument by substituting the gamma function:

$$\binom{\alpha}{m} = \frac{\Gamma(\alpha + 1)}{\Gamma(m + 1)\Gamma(\alpha - m + 1)}, \quad (1)$$

yielding the *Grünwald-Letnikov derivative*:

$$\frac{d^\alpha f}{dt^\alpha}(t) = \lim_{\Delta t \rightarrow 0} \frac{1}{(\Delta t)^\alpha} \sum_{j=0}^{\infty} (-1)^j \binom{\alpha}{j} f(t + (\alpha - j)\Delta t). \quad (2)$$

If  $\Delta t \ll 1$  and  $t = m\Delta t$ , then the quantity  $\alpha\Delta t$  in the argument of  $f$  can be neglected, and assuming initial conditions of zero, the approximation becomes

$$\frac{d^\alpha f}{dt^\alpha}(t) \approx \frac{1}{(\Delta t)^\alpha} \sum_{j=0}^m (-1)^j \binom{\alpha}{j} f(t - j\Delta t),$$

which is an efficient way to formulate solutions of fractional-order differential equations.

A notable difference between fractional- and integer-order derivatives is that fractional-order derivatives cannot be computed from local information only. The summation in Equation 2 is evidence that all past values of a function are part of the computation of its fractional derivative.

## III. MATHEMATICAL ANALYSIS

This section summarizes the discussion from [2] concerning the damaged and undamaged systems.

### A. Undamaged System

The tree formation of Figure 1 is comprised of two types of transfer functions at the component level. The transfer function from the  $x_{11}$  node to the  $x_{21}$  node is  $G_1(s) = 1/k$ , and that from the  $x_{11}$  node to the  $x_{22}$  node is  $G_2(s) = 1/(bs)$ . The formation is built on parallel and series connections of these two relationships. To formulate the transfer function of the formation as a whole, *i.e.*,  $G(s) = (X_{11}(s) - X_{\text{last}}(s))/U(s)$  with  $u(t)$  the input force generated by the formation structure, then the component transfer functions are combined as specified by the system to give

$$G(s) = \frac{1}{\frac{1}{G_1(s) + \frac{1}{\frac{1}{G_1(s)+\dots + G_2(s)+\dots}}} + \frac{1}{G_2(s) + \frac{1}{\frac{1}{G_1(s)+\dots + G_2(s)+\dots}}}.$$

In the limit of infinitely many generations, self-similarity prescribes that the transfer function from any node to the last generation is equal to that from the first node to the last generation. This is denoted by  $G_\infty(s)$ , leading to the equation

$$G_\infty(s) = \frac{1}{\frac{1}{G_1(s) + G_\infty(s)} + \frac{1}{G_2(s) + G_\infty(s)},$$

which yields  $G_\infty(s) = \sqrt{G_1(s)G_2(s)}$ . This is true regardless of what  $G_1(s)$  and  $G_2(s)$  are; however, for this system, the limiting transfer function is

$$G_\infty(s) = \frac{1}{\sqrt{kbs}}. \quad (3)$$

Since  $s$  is the Laplace transform of the derivative operator, the square root of  $s$  represents 1/2-order dynamics.

This order result can be confirmed with the identification procedure developed in this research effort. The identified transfer function is given by

$$F(s) = \frac{3189}{s^{13/6} + \dots + 4289s^{1/2} + 102s^{1/3} + \dots + 22}. \quad (4)$$

The coefficient of the term of order 1/2 is an order of magnitude higher than that of any other; this means that order 1/2 is dominant, so the theoretical expectation is met. The details of how this result is obtained are given in the following sections.

As discussed in [1] and [2], Equation 2 can be used to generate a time-domain response of the last generation in the system,  $x_{\text{last}}$ , under some displacement of  $x_{11}$  from zero. In particular,

$$\dot{x}_{11} = \begin{cases} t, & 0 \leq t < 1 \\ 2-t, & 1 \leq t < 2 \\ 0, & t \geq 2 \end{cases},$$

and an expression of Newton's second law on the last generation using Equation 3 gives

$$ms^2 X_{\text{last}}(s) = \sqrt{kbs}(X_{11}(s) - X_{\text{last}}(s)),$$

or in the time domain,

$$m \frac{d^2 x_{\text{last}}}{dt^2}(t) + \sqrt{kb} \frac{d^{1/2} x_{\text{last}}}{dt^{1/2}}(t) = \sqrt{kb} \frac{d^{1/2} x_{11}}{dt^{1/2}}(t).$$

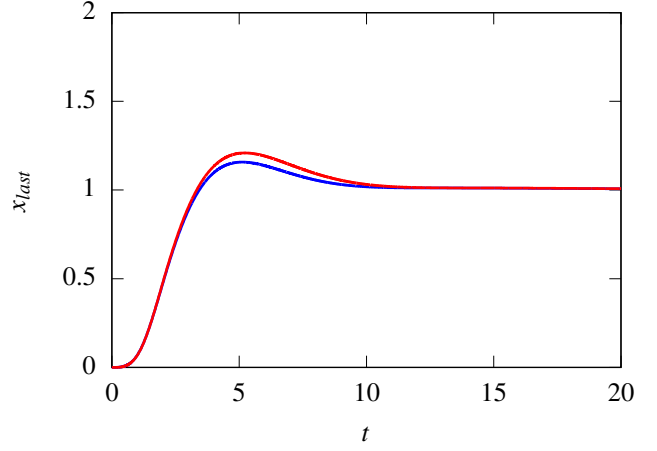


Fig. 4. Response of fractional system of order 0.66 (blue) and response of full system with damage to spring (red).

Equation 2 can be manipulated to determine  $x_{\text{last}}$  at  $t = n\Delta t$ . This expression is

$$\begin{aligned} x_{\text{last}}(n\Delta t) \approx & \left( \frac{1}{\frac{m}{(\Delta t)^2} + \frac{\sqrt{kb}}{\sqrt{\Delta t}}} \right) \\ & \times \left[ \frac{m}{(\Delta t)^2} (2x_{\text{last}}((n-1)\Delta t) - x_{\text{last}}((n-2)\Delta t)) \right. \\ & - \frac{\sqrt{kb}}{\sqrt{\Delta t}} \sum_{j=1}^n (-1)^j \binom{1/2}{j} x_{\text{last}}((n-j)\Delta t) \\ & \left. + \frac{\sqrt{kb}}{\sqrt{\Delta t}} \sum_{j=0}^n (-1)^j \binom{1/2}{j} x_{11}((n-j)\Delta t) \right], \end{aligned} \quad (5)$$

and it can be evaluated iteratively to compute the response.

In [1] and [2], the fractional-order response just described is compared to the response of the unapproximated full system with eight generations, both having the constants  $k = 2$ ,  $b = 1$ , and  $m = 1$ . The solution of the fractional equation is shown to be a strong approximation for that of the full system, which requires 255 second-order differential equations to simulate.

### B. Damaged System

Consider the version of the system with the leftmost spring being damaged, or having a stiffness different from its nominal value;  $k_d = 0.2$  instead of 2. This system shifts in phase from  $-45^\circ$  to approximately  $-60^\circ$  at  $\omega \approx 1$  rad/s, illustrated in Figure 2, suggesting approximately 2/3-order dynamics. The magnitude at that frequency is shifted from the undamaged case by about 7 dB, which means that the force produced by the network is reduced by a factor of 0.45.

The interpretation that the order of the system has changed can be affirmed by comparing the time-domain responses of a seven-generation system with the same damaged spring and a fractional-order system with order 0.66, as in Figure 4. The full system is as in the other case, except that  $k_d = 0.2$ .

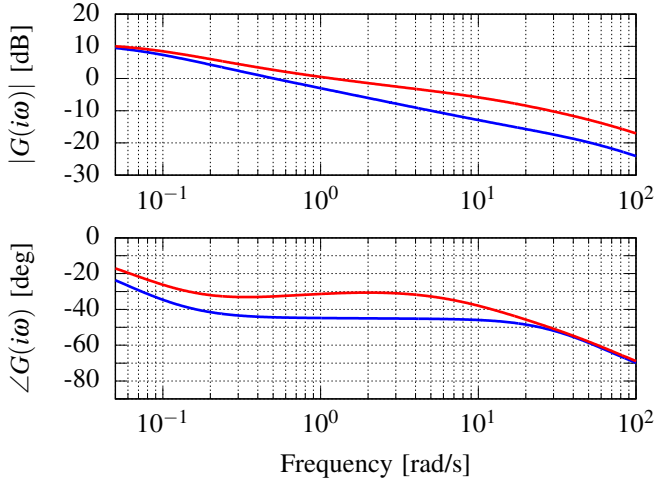


Fig. 5. Frequency responses for undamaged system (blue) and damaged system with  $b_d = 0.1$  (red).

The response of the fractional-order system is given by Equation 5, except with order 0.66 (so all instances of  $1/2$ , including exponents and binomial coefficient arguments, become 0.66) and multiplying the force by a factor of  $M = -7$  dB to match the magnitude shift.

Following from Figure 4, it is evident that the change  $k \rightarrow k_d$  produces a corresponding change in the system's order, from  $1/2$  to  $2/3$ . This implies that monitoring of the order may reveal changes to the operational status of the system.

The final example from [2] is the tree system with damage to the leftmost damper; its constant is reduced from  $b = 1$  to  $b = 0.1$ . Figure 5 shows this system's frequency response in red. Opposite to the case of the damaged spring, this response shows a *decrease* in order, from  $1/2$  to approximately  $1/3$ . As in the damaged spring case, the magnitude at 1 rad/s is decreased, in this case by about  $10^{-4/20}$ . The time-domain response is found by Equation 5 with order 0.33 and  $M = 10^{-4/20}$ . This fractional-order response is given in Figure 6; as in the other examples, agreement with the full tree system is achieved.

#### IV. IDENTIFICATION PROCEDURE

This section explains the system identification method of [10] and modifications for generality that were made in this research effort. In the reference, the frequency response given in the data is  $G(s)$ . The model to be found is of the form

$$F(s) = \frac{K_0 B(s)}{s^{d_0} A(s)} = \frac{K_0 \sum_{k=0}^n b_k s^{\beta_k}}{s^{d_0} \sum_{k=0}^d a_k s^{\alpha_k}}$$

where  $a_0 = b_0 = 1$ ,  $\alpha_0 = \beta_0 = 0$ , and  $\alpha_k, \beta_k \in \mathbb{R}$ . This is restrictive in the sense that the resulting transfer function must take the form

$$F(s) = \frac{K_0 b_n s^{\beta_n} + \dots + b_1 s^{\beta_1} + 1}{s^{d_0} a_d s^{\alpha_d} + \dots + a_1 s^{\alpha_1} + 1}, \quad (6)$$

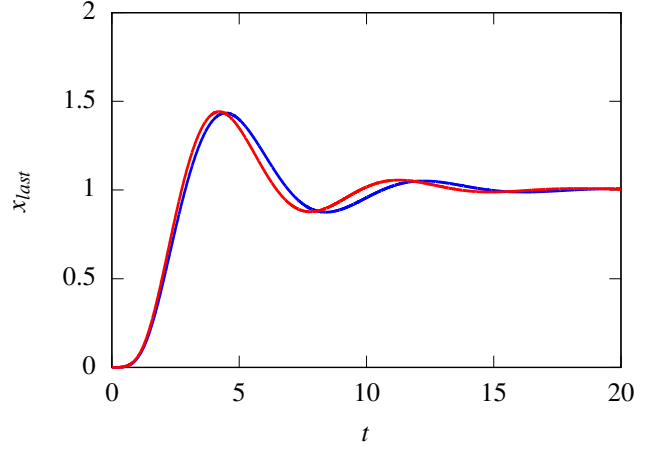


Fig. 6. Response of fractional system of order 0.33 (blue) and response of full system with damage to damper (red).

so there is always a constant term in the numerator. The constants  $K_0$  and  $d_0$  establish a gain and a pole at the origin, allowing for some flexibility. However, these constants must be set before the optimization takes place, so they cannot be considered part of the identification.

This approach is suitable for solution by the simplex method, so the answer is a state vector:

$$w = [b_1 \ \dots \ b_n \ a_1 \ \dots \ a_d \ w_{n+d+1}]^T,$$

where  $w \geq 0$ . The last entry,  $w_{n+d+1}$ , is included in the state vector for the purposes of the linear constraints, which set a bound on the error metric

$$R(j\omega) = \frac{(j\omega)^{d_0}}{K_0} A(j\omega) (F(j\omega) - G(j\omega)),$$

specifically its  $L^\infty$ -norm,

$$\|R(j\omega_i)\| = \max(|\operatorname{Re}(R(j\omega_i))|, |\operatorname{Im}(R(j\omega_i))|).$$

Given data at  $m$  frequencies, there is a list of  $2m$  real and imaginary parts ( $m$  each) of  $R(j\omega)$ , and the method of [10] minimizes the largest absolute value of the numbers in this list. This iterative problem is cast as the minimization of one variable, so the objective function is linear, lending itself to the simplex method.

In contrast, the procedure in this work minimizes an objective function  $J$  equal to

$$\sum_{i=1}^m \left| \left( \sum_{k=0}^n b_k (j\omega_i)^{\beta_k} \right) - \frac{(j\omega_i)^{d_0}}{K_0} \left( \sum_{k=0}^d a_k (j\omega_i)^{\alpha_k} \right) G(j\omega_i) \right|,$$

which is equivalent to

$$J = \sum_{i=1}^m \left| B(j\omega_i) - \frac{(j\omega_i)^{d_0}}{K_0} A(j\omega_i) G(j\omega_i) \right|$$

and, in turn,

$$J = \sum_{i=1}^m \left| \frac{(j\omega_i)^{d_0}}{K_0} A(j\omega_i) (F(j\omega_i) - G(j\omega_i)) \right|.$$

Therefore, instead of considering only the largest real or imaginary part of error between the data and the identified model, this procedure minimizes

$$J = \sum_{i=1}^m \sqrt{(\operatorname{Re}(R(j\omega_i)))^2 + (\operatorname{Im}(R(j\omega_i)))^2}.$$

The coefficients

$$v = [b_1 \ \cdots \ b_n \ a_1 \ \cdots \ a_d]^T$$

are determined by the MATLAB function `fmincon` with the corresponding interior-point algorithm. As a result of this choice of optimization, none of the coefficients terminate at zero, so the resulting transfer functions have terms for every order in  $\alpha$  and  $\beta$ . This shows the degree of dominance of each order relative to the others.

The function `fmincon` is for constrained optimization, so it is necessary to establish constraints. A natural choice would be to require that all entries in the solution vector  $v$  be greater than or equal to zero. However, the set of constraints in this procedure is slightly different: all entries of  $v \geq 0$ , except  $a_1, b_1 \geq -1$ . These two coefficients correspond to  $s^0$  terms ( $\alpha_1 = \beta_1 = 0$ ) to allow for cancellation of the built-in 1's in the numerator and denominator of Equation 6, generalizing the form of the resulting transfer function.

## V. RESULTS

The undamaged tree system has a theoretical transfer function of  $s^{-1/2}$ , while the cases of damage to the first spring and first damper give rise to transfer functions of  $s^{-2/3}$  and  $s^{-1/3}$ , respectively. This is seen most clearly in the Bode plots for these systems (Figures 2 and 5), which feature prominent frequency bands of approximate phase  $-45^\circ$ ,  $-60^\circ$ , and  $-30^\circ$ . To verify the system identification procedure, these transfer functions are sought from tree system data sampled over these frequency bands only. In the style of [10],  $\alpha_k$  (with  $k$  starting at 1) is chosen to be  $0, 1/6, \dots, 13/6$  so as to make over two integer orders of possible solutions available. However,  $\beta_k$  is set to 0 only to allow comparison between the expected and computationally obtained results.

It is hypothesized that the system identification procedure will return transfer functions matching theoretical expectation. Therefore, the starting points of the optimizations are

$$\begin{aligned} v_0 &= [b_1 \ a_1 \ a_2 \ \cdots \ a_{14}] \\ &= [0 \ -1 \ 0 \ \cdots \ 0 \ 1 \ 0 \ \cdots \ 0]^T, \end{aligned}$$

where the 1 is placed in a different entry for each starting point:  $a_3$  for  $s^{-1/3}$ ,  $a_4$  for  $s^{-1/2}$ , and  $a_5$  for  $s^{-2/3}$ . In general, if the 1 is placed in  $a_k$  with  $k > 1$ , the corresponding transfer function is  $s^{-(k-1)/6}$ . A detailed formulation of the starting point following from this choice of  $v_0$  is

$$F_0(s) = \frac{0s^0 + 1}{s^{(k-1)/6} - s^0 + 1} = \frac{1}{s^{(k-1)/6}}.$$

The following are the system identification results. The transfer functions are scaled so that the leading-order coefficient in the denominator is 1. For the undamaged tree

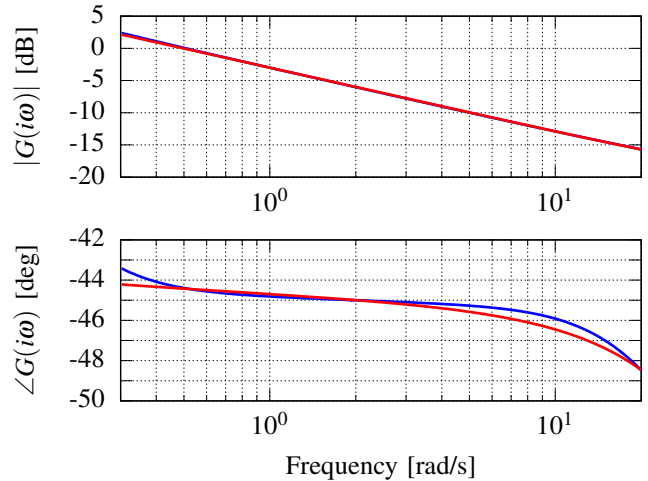


Fig. 7. Actual (blue) and identified (red) frequency responses for the undamaged system.

with eight generations of robots and 19 frequencies ( $m = 19$ ) logarithmically spaced from  $10^{-0.5}$  to  $10^{1.3}$  rad/s,  $F(s)$  is given in Equation 4. As stated previously, order 1/2 dominates; this corroborates the visual interpretation of the frequency response from [2]. The comparison of  $F(s)$  to  $G(s)$  is shown in Figure 7.

For the tree formation with damage to the first spring,  $m = 29$ , and a frequency band from  $10^{-0.8}$  to  $10^2$  rad/s,

$$F(s) = \frac{17927}{s^{13/6} + \cdots + 9466s^{2/3} + 1658s^{1/2} + \cdots + 470}.$$

Order 2/3 is prominent, but its coefficient is not an order of magnitude above all of the others. Still, it is over five times the next largest, so an integrator approximation for this system would be of order 2/3, as expected. Despite the wide frequency band, the identified transfer function yields a frequency response that matches the data well, as shown in Figure 8.

When the damage is instead to the first damper, and  $m = 19$  with a frequency band from  $10^{-0.8}$  to  $10^1$  rad/s,

$$F(s) = \frac{1638}{s^{13/6} + \cdots + 124s^{1/2} + 1246s^{1/3} + \cdots + 31}.$$

Here, the coefficient of order 1/3 is an order of magnitude greater than the others, so that order is dominant. This result's frequency response is shown alongside the tree formation's in Figure 9. In all cases, the frequency bands are chosen experimentally to capture the dynamics of interest.

As shown, the resulting transfer functions  $F(j\omega)$  match the magnitudes of  $G(j\omega)$  almost exactly, but for some frequencies, they have a few degrees' error in phase. A reason for this is that, because the numerator is required to be constant so as to illustrate the dominant orders,  $F(s)$  cannot have zeros. Nonminimum phase dynamics are never present, so the phase trajectory of  $F(j\omega)$  can only decrease as frequency increases.

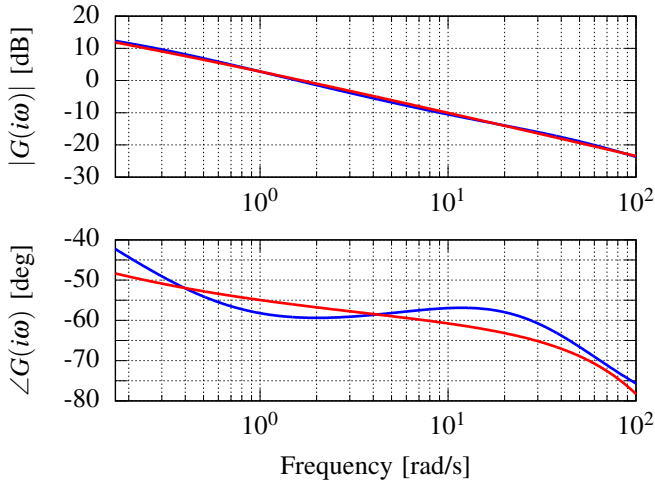


Fig. 8. Actual (blue) and identified (red) frequency responses for the tree system with damage to the first spring.

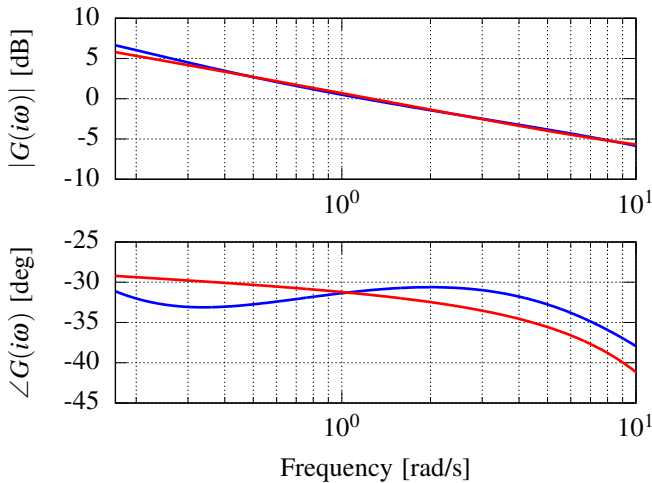


Fig. 9. Actual (blue) and identified (red) frequency responses for the tree system with damage to the first damper.

## VI. CONCLUDING REMARKS

This paper has introduced a new identification method for fractional-order systems. The method shows which orders of dynamics are most present in a system's frequency response. In the context of a robot formation undergoing damage, this method has shown itself able to track a change in order. As a monitoring tool for systems in general, this may be a valuable indicator that the operational status has changed.

Future efforts should naturally include testing the method on other damage cases and systems. At present, altering the frequency window of interest in the identification can affect the strength of the result. The best frequency window in which to sample will not always be known, so perhaps an outer optimization loop to narrow and translate the window would strengthen the results and thus enhance the reliability of the method. However, considering the variety of systems to which mechanical models are applied, it is important to

preserve information from systems that may exhibit response behavior of multiple orders simultaneously.

The neatness of the damage results in the robot formation example suggests a mathematical framework relating physical damage to a system and effects on its governing equation. The details of this framework largely remain unclear, but it is likely that some insights may be found through perturbation analysis. These insights and improvements to the method will bring about a greater scope of application for extracting system information from fractional-order behavior.

## REFERENCES

- [1] Bill Goodwine. Modeling a multi-robot system with fractional-order differential equations. In *Proceedings of the IEEE International Conference on Robotics and Automation*, pages 1763–1768, 2014.
- [2] Kevin Leyden and Bill Goodwine. Using fractional-order differential equations for health monitoring of a system of cooperating robots. In *Proceedings of the IEEE International Conference on Robotics and Automation*, 2016.
- [3] N. Heymans and J.C. Bauwens. Fractal rheological models and fractional differential equations for viscoelastic behavior. *Rheologica Acta*, 33:210219, 1994.
- [4] Jason Mayes. *Reduction and Approximation in Large and Infinite Potential-Driven Flow Networks*. PhD thesis, University of Notre Dame, 2012.
- [5] Tom T. Hartley and Carl F. Lorenzo. Fractional-order system identification based on continuous order-distributions. *Signal processing*, 83(11):2287–2300, 2003.
- [6] Shantanu Das. *Functional fractional calculus*. Springer Science & Business Media, 2011.
- [7] Da-Yan Liu, Taous-Meriem Laleg-Kirati, Olivier Gibaru, and Wilfrid Perruquetti. Identification of fractional order systems using modulating functions method. In *American Control Conference (ACC), 2013*, pages 1679–1684. IEEE, 2013.
- [8] Arun Narang, Sirish L. Shah, and T. Chen. Continuous-time model identification of fractional-order models with time delays. *IET Control Theory & Applications*, 5(7):900–912, 2011.
- [9] Shengxi Zhou, Junyi Cao, and Yangquan Chen. Genetic algorithm-based identification of fractional-order systems. *Entropy*, 15(5):1624–1642, 2013.
- [10] Alain Oustaloup. *La dérivation non entière*. Hermes, 1995.
- [11] Wei Ren, Randal W. Beard, and Ella M. Atkins. Information consensus in multivehicle cooperative control. *IEEE Control Systems Magazine*, pages 71–82, April 2007.
- [12] J. Alexander Fax and Richard M. Murray. Information flow and cooperative control of vehicle formations. *IEEE Transactions on Automatic Control*, 49(9):1465–1476, 2004.
- [13] N.E. Leonard and E. Fiorelli. Virtual leaders, artificial potentials, and coordinated control of groups. In *Proceedings of the 40th IEEE Conference on Decision and Control*, pages 2968–2973, December 2001.
- [14] Aavek K. Das, Rafael Fierro, Vijay Kumar, James P. Ostrowski, John Spletzer, and Camillo J. Taylor. A vision-based formation control framework. *IEEE Transactions on Robotics and Automation*, 18(5):813–825, 2002.
- [15] Richard M Murray. Recent research in cooperative control of multivehicle systems. *Journal of Dynamic Systems Measurement and Control*, 129(5):571, 2007.
- [16] Yongcan Cao, Wenwu Yu, Wei Ren, and Guanrong Chen. An overview of recent progress in the study of distributed multi-agent coordination. *Industrial Informatics, IEEE Transactions on*, 9(1):427–438, 2013.
- [17] M. Brett McMickell and Bill Goodwine. Reduction and non-linear controllability of symmetric distributed systems. *International Journal of Control*, 76(18):1809–1822, 2003.
- [18] M. Brett McMickell and Bill Goodwine. Motion planning for nonlinear symmetric distributed robotic formations. *The International journal of robotics research*, 26(10):1025–1041, 2007.
- [19] Bill Goodwine and Panos J. Antsaklis. Multi-agent compositional stability exploiting system symmetries. *Automatica*, pages 3158–3166, 2013.

- [20] M. Brett McMickell and Bill Goodwine. Reduction and non-linear controllability of symmetric distributed systems with drift. In *Proceedings of the IEEE International Conference on Robotics and Automation*, pages 3454–3460, 2002.
- [21] Keith B. Oldham and Jerome Spanier. *The Fractional Calculus*. Academic Press, New York, 1974.
- [22] Dumitru Baleanu, José António Tenreiro Machado, and Albert C. J. Luo. *Fractional Dynamics and Control*. Springer Publishing Company, Incorporated, 2011.
- [23] Manuel Duarte Ortigueira. *Fractional Calculus for Scientists and Engineers*, volume 84 of *Lecture Notes in Electrical Engineering*. Springer, 2011.
- [24] M.D. Ortigueira. An introduction to the fractional continuous-time linear systems: the 21st century systems. *Circuits and Systems Magazine, IEEE*, 8(3):19–26, 2008.
- [25] J. Tenreiro Machado, Virginia Kiryakova, and Francesco Mainardi. Recent history of fractional calculus. *Communications in Nonlinear Science and Numerical Simulation*, 16(3):1140 – 1153, 2011.
- [26] Yongcan Cao and Wei Ren. Distributed formation control for fractional-order systems: Dynamic interaction and absolute/relative damping. *Systems & Control Letters*, 59(34):233 – 240, 2010.
- [27] Yongcan Cao, Yan Li, Wei Ren, and Yang Quan Chen. Distributed coordination of networked fractional-order systems. *Systems, Man, and Cybernetics, Part B: Cybernetics, IEEE Transactions on*, 40(2):362–370, 2010.
- [28] Bill Goodwine. Fractional-order dynamics in a random, approximately scale-free network of agents. In *Proceedings of the IEEE Conference on Control Automation Robotics & Vision*, pages 1581–1586, 2014.
- [29] Bill Goodwine and Kevin Leyden. Recent results in fractional-order modeling for multi-agent systems and linear friction welding. Extended abstract, 8th Vienna International Conference on Mathematical Modelling, 2015.